ELSEVIER

Structure of cholest-5-en-3β-oxy-5-bromopentane by single-crystal X-ray diffraction at 130 K

Yamuna Krishnan-Ghosh[a], R. Srinivasa Gopalan[b], G.U. Kulkarni[b],
Santanu Bhattacharya[a],*

[a]*Department of Organic Chemistry, Indian Institute of Science, Bangalore 560 012, India*
[b]*Chemistry and Physics of Materials Unit, Jawaharlal Nehru Centre For Advanced Scientific Research, Jakkur, Bangalore 560 064, India*

Abstract

Cholest-5-en-3β-oxy-5-bromopentane (**1**) and cholest-5-en-3β-oxy-11-bromoundecane (**2**), key precursors for the synthesis of novel cationic amphiphiles based on cholesterol, have been synthesized and characterized by ^{1}H-NMR spectroscopy and X-ray crystallography. Thermal disorder and effect of length of the bromoalkyl segment on the crystal structure have been investigated. Possible molecular level explanation of the unusual alternating s-*trans*−*gauche* conformation of the bromopentyl side chain of (**1**) has been presented. © 2001 Elsevier Science B.V. All rights reserved.

Keywords: X-ray crystallography; Cholesteryl ether; Thermal disorder; Side-chain

1. Introduction

We have been interested in the design of novel cationic lipids due to their utility in liposome-mediated DNA transfection [1,2]. Amphiphilic ether derivatives of cholesterol are gaining much importance due to the recent finding that they are more potent than their ester or urethane counterparts in gene delivery [3]. However, these biomaterials are active only as liposomal membrane formulations. Membrane properties such as rigidity, permeability, conductivity and even in vivo tissue distribution are profoundly affected upon incorporation of cholesterol or its derivatives [4–9]. The mode of packing of these cholesteryl derivatives in membranes holds the key to understanding why ether derivatives of cholesterol are more active than any other derivatives of cholesterol. It has been postulated that the packing of cholesteryl monomers in their crystals is analogous to their packing in membranes [10]. Indeed, several theoretical treatments of cholesterol in membranes [11] invoke crystal parameters of analogous cholesterol derivatives [12]. Though several reports on cholesteryl esters and carbonates exist [13–17], apart from cholesteryl methyl ether [18], which affords no information on the crucial *O*-alkyl substituent, there are no reports of single-crystal X-ray diffraction studies on ether based derivatives of cholesterol.

In this paper, we report the synthesis of two key precursors of these cationic cholesteryl ether derivatives, cholest-5-en-3β-oxy-5-bromopentane (**1**) and cholest-5-en-3β-oxy-11-bromoundecane (**2**). Suitable quality crystals were grown from these materials. Single-crystal X-ray diffraction analysis reveal that these crystals remain in a thermally disordered state at 298 K. However, the crystal structure of

---

* Corresponding author. Also at: Chemical Biology Unit of JNCASR, Bangalore 560 012, India. Fax: +91-80-3600529.
E-mail address: sb@orgchem.iisc.ernet.in (S. Bhattacharya).

cholest-5-en-3β-oxy-5-bromopentane (**1**) at 130 K could be satisfactorily solved, which provide pertinent details about the packing of this class of molecules in a crystalline environment.

2. Experimental

2.1. Materials and general methods

Cholesterol was purchased from Sigma. All other reagents and solvents were obtained from best known commercial sources and were purified, dried or freshly distilled as required according to the specified literature procedure [19]. Cholesterol tosylate was synthesized using a literature procedure [20]. Thin layer chromatography was performed on silica gel-G (Merck) by visualization in iodine chamber and preparative column chromatography was performed on silica gel (60–120 mesh).

2.2. Synthesis

Melting points were recorded in open capillary tubes on a Büchi model 510 melting point apparatus and are uncorrected. ^{1}H-NMR spectra (TMS as internal standard) were recorded on a JEOL-JANL-LA-300 NMR spectrometer. Chemical shifts (δ) are reported in ppm downfield from the internal standard. IR spectra were recorded on a JASCO 410 FT/IR spectrometer and are reported in wave numbers (cm^{-1}). Microanalyses were performed on a Carlo Erba elemental analyzer model 1106.

Cholest-5-en-3β-oxy-pentan-5-ol (**3**). To a suspension of cholest-5-ene-3β-tosylate (2.0 g, 3.7 mmol) in anhydrous dioxane (9 ml) was added 1,5-pentanediol (5 ml) and the mixture was stirred under reflux for 4 h in dry nitrogen atmosphere. The solution was cooled and the solvent removed in vacuo. The white residue was partitioned between CHCl$_3$ (20 ml) and water (20 ml) and washed sequentially with saturated NaHCO$_3$ (2×10 ml), water (10 ml) and saturated brine (10 ml), dried over anhydrous Na$_2$SO$_4$ and the solvent removed in vacuo. The residue was purified by column chromatography on silica gel (60–120 mesh) using 1:9 ethyl acetate/hexane to give a white solid (1.4 mg, 2.96 mmol, 80%) m.p.: 101–102°C. IR (KBr, cm^{-1}): 3385 (br, OH), 2933, 2860, 1466, 1377, 1093. ^{1}H-NMR

(CDCl$_3$, 300 MHz); δ: 0.67 (3H, s), 0.85–1.59 (39H, m), 1.81–2.32 (8H, m), 3.04–3.12 (1H, m), 3.43 (2H, t, $J = 4.5$ Hz), 3.62 (2H, t, $J = 4.5$ Hz), 5.29 (1H, d, $J = 4.5$ Hz). LRMS: 473 (M$^+$). C$_{32}$H$_{56}$O$_2$1/2C$_6$H$_{14}$: C, 81.48; H, 12.31; Found: C, 81.86; H, 12.18.

Cholest-5-en-3β-oxy-5-bromopentane (**1**): To a cooled solution of (**2**) (1.0 g, 2.11 mmol) in dry CH$_2$Cl$_2$ (20 ml), was added triphenylphosphine (0.663 g, 2.53 mmol, 1.2 equiv.). To this, a solution of CBr$_4$ (0.844 g, 2.53 mmol, 1.2 equiv.) in dry CH$_2$Cl$_2$ was added and allowed to stir at 0°C for 3 h. The reaction was continued till the complete disappearance of starting material as checked by TLC. The reaction mixture was washed in a separatory funnel, respectively, with water (20 ml), brine (20 ml) and finally dried over anhydrous Na$_2$SO$_4$. The solvent was evaporated and the residue was purified by repeated crystallization from dry acetone to give white crystals (1.09 g, 2.05 mmol, 97%) m.p.: 62°C IR (KBr, cm^{-1}): 2934, 2867, 1466, 1375, 1097. ^{1}H-NMR (CDCl$_3$, 300 MHz); δ: 0.67 (3H, s), 0.86–1.55 (39H, m), 1.83–2.33 (8H, m), 3.10 (1H, m), 3.42 (2H, t, $J = 4.5$ Hz), 3.48 (2H, t, $J = 8.0$ Hz), 5.30 (d, $J = 4.5$ Hz, 1H). LRMS: 536 (M$^+$ + 2, 2%), 534 (M$^+$, 2%). Anal. Calcd. for C$_{32}$H$_{55}$OBr: C, 71.74; H, 10.35; Found: C, 71.59; H, 10.67.

Cholest-5-en-3β-oxy-5-bromoundecane (**2**): To a suspension of cholest-5-ene-3β-tosylate (2.0 g, 3.7 mmol) in anhydrous dioxane (9 ml) was added 11-bromoundecanol (5.0 g, 20 mmol) and the mixture was stirred under reflux for 7 h in an inert atmosphere. The solution was cooled and the solvent removed in vacuo. The white residue was partitioned between CHCl$_3$ (20 ml) and water (20 ml) and washed sequentially with saturated NaHCO$_3$ (2×10 ml), water (10 ml) and saturated brine (10 ml), dried over anhydrous Na$_2$SO$_4$ and the solvent removed in vacuo. The residue was purified by column chromatography on silica gel (60–120 mesh) using 1:19 ethyl acetate/hexane to give a white solid (1.8 mg, 2.91 mmol, 78%) which was crystallized from dry acetone. m.p: 68–70°C. IR (KBr, cm^{-1}): 2933, 2860, 1466, 1377, 1093. ^{1}H-NMR (CDCl$_3$, 300 MHz); δ: 0.67 (3H, s), 0.85–1.66 (51H, m), 1.87–2.33 (8H, m), 3.03–3.11 (1H, m), 3.39 (2H, t, $J = 4.5$ Hz), 3.60 (2H, t, $J = 4.5$ Hz), 5.28 (1H, d, $J = 4.5$ Hz). LRMS: 620 (M$^+$ + 2), 618

Table 1
Crystal data and experimental crystallographic details

Empirical formula	$C_{32}H_{55}BrO$
Formula weight	535.67
Temperature	130(2) K
Wavelength	0.71073 Å
Crystal system	Monoclinic
Space group	P 2(1)
Unit cell dimensions	$a = 12.1900(3)$ Å; $\alpha = 90°$.
	$b = 8.9726(2)$ Å;
	$\beta = 92.3460(10)°$.
	$c = 13.6994(4)$ Å $\gamma = 90°$.
Volume (Z)	1497.13(7) Å^3, 2
Density (calculated)	1.188 Mg/m^3
Absorption coefficient	1.394 mm^{-1}
$F(000)$	580
Crystal size	$0.3 \times 0.2 \times 0.2$ mm^3
On the diffractometer:	
θ range for data collection	1.49–23.41°
Index ranges	$-13 \leq h \leq 13$, $-9 \leq k \leq 9$,
	$-15 \leq l \leq 11$
Reflections collected	6433
Independent reflections	4189 [$R(\text{int}) = 0.0203$]
Refinement method	Full-matrix least-squares on F^2
Data/restraints/parameters	4189/1/307
Goodness-of-fit on F^2	1.077
Final R indices [$I > 2\sigma_I$]	$R1 = 0.0449$, $wR2 = 0.1221$
R indices (all data)	$R1 = 0.0492$, $wR2 = 0.1322$
Absolute structure parameter	0.015(11)
Largest diff. peak and hole	0.811 and -0.480 e Å^{-3}

(M$^+$). $C_{38}H_{67}OBr0.25H_2O$: C, 73.1; H, 10.9; Found: C, 72.8; H, 10.98.

2.3. X-ray crystallography

Crystals of **1** and **2** were obtained from acetone. High-quality crystal of respective compounds was chosen after examination under an optical microscope. X-ray diffraction intensities were measured by ω-scans using a ω Siemens three-circle diffractometer attached with a CCD area detector and a graphite monochromator using a stream of cold nitrogen gas from a vertical nozzle and this temperature was maintained throughout the data collection. The unit cell parameters and the orientation matrix of the crystal were initially determined using ~60 reflections from 25 frames collected over a small ω scan of ~7.4° sliced at 0.3° interval. A hemisphere of reciprocal space was then collected in two shells using SMART software [21] with 2θ settings of the detector at 28°. Data reduction was performed using the SAINT program [22] and the orientation matrix along with the detector and the cell parameters were refined for every 40 frames on all the measured reflections. The various experimental details are listed in Table 1. The phase problem was solved by direct methods and
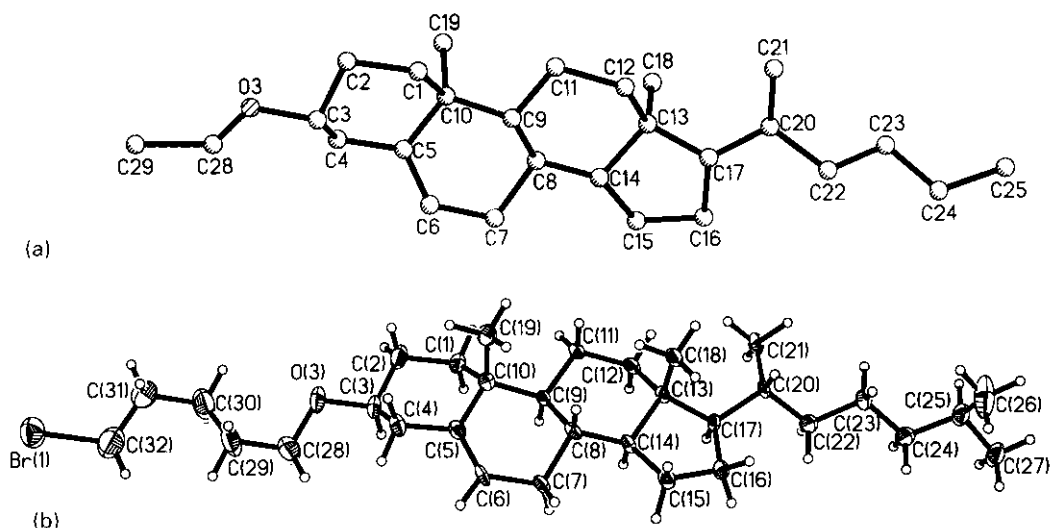

Fig. 1. A: Crystal structure of **1** at 298 K. B: ORTEP plot of **1** at 130 K with the atom numbering scheme.
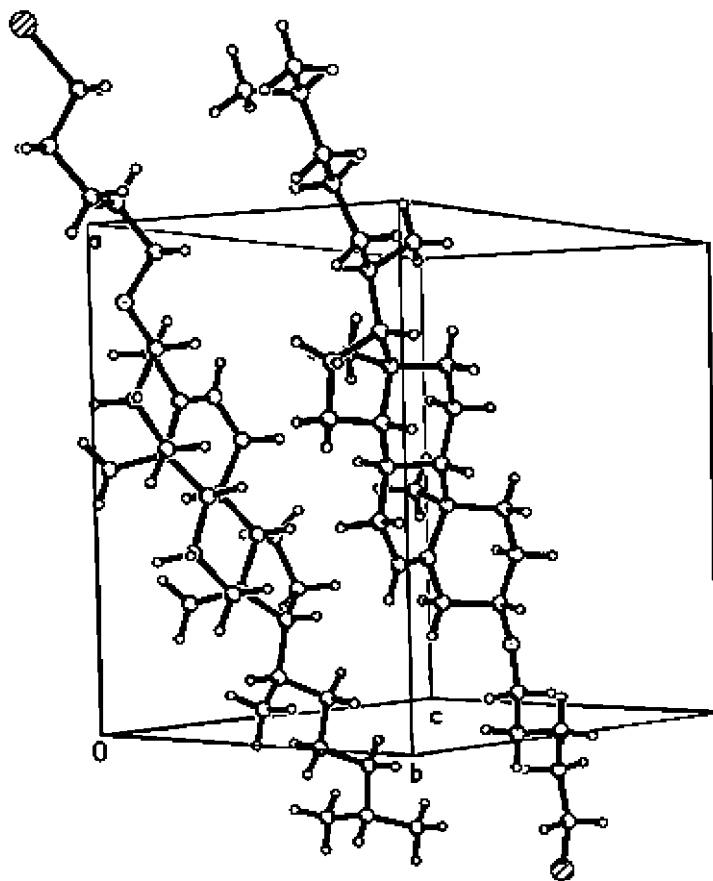
Fig. 2. Unit cell packing of **1** at 130 K.

the non-hydrogen atoms were refined anisotropically, by means of the full-matrix least-squares using SHELXTL program [22]. All the hydrogens were fixed and the temperature factors of the hydrogens were refined isotropically.

3. Results and discussion

First the crystal structure of **1** was determined at 298 K. Subsequently, the diffraction data revealed a structure (as shown in Fig. 1A) with large apparent thermal vibrational averaging caused possibly due to conformational disordering. This obscured atomic details in the terminal portion of the isopentyl steroid

side chain as well as that of the *n*-bromopentyl side chain at the β-oxygen. We then decided to collect X-ray diffraction data at low temperature (130 K). Indeed, this provided sufficiently detailed and accurate information about the structure prior to the onset of several thermal-averaging effects. This is presented as an ORTEP drawing in Fig. 1B. The relevant crystal data and experimental crystallographic details are presented in Table 1.

Molecule **1** crystallized in the *P*2(1) space group (Fig. 1B). It was clear that the steroidal portion of these molecules behaved as a rigid body [23] in contrast to the thermal motions in the *n*-alkyl side chain attached to O(3). Bond distances and bond angles at 130 K were consistent with those found in
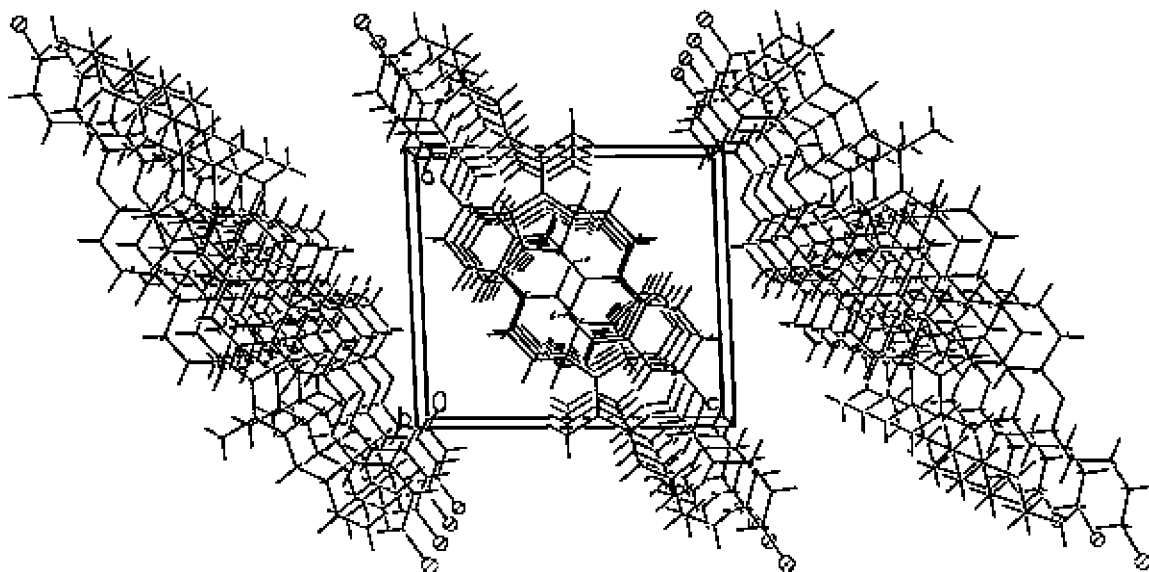
Fig. 3. Molecular packing of **1** at 130 K looking down the *b*-axis.

crystal structure of cholesteryl acetate determined at 123 K by Sawzik et al. [24]. At low temperature (130 K), the average least squares estimated standard deviation for bond distances is 0.095 Å and 4.0° for bond angles with the structure shown in Fig. 1A while these values are 0.008 Å and 0.8° with the structure shown in Fig. 1B. The tetracyclic-fused ring skeletons, as they appear in Fig. 1A and 1B, show similar conformations. A least-squares fit for the superposition [25] of the C(1)–C(19) fragment from the two structures (Fig. 1A and 1B) results in an rms displacement of 0.095 Å. The effective length of the steroid moiety taken as the C(3)–C(16) distance for the structure of **1** determined at 298 and 130 K are 8.988 and 8.968 Å, respectively. A measure of the twist within the ring systems is given by the C(19)–C(10)–C(13)–C(18) torsion angle which for **1** at 298 and 130 K has a value of 9.0 and 9.6°, respectively. The rotation about the ether linkage at 130 K as given by the torsion angle C(2)–C(3)–O(3)–C(28) was found to be 155.6°. The unit cell shown for the compound **1** at 130 K (Fig. 2) contains two molecules arranged in head-to-tail fashion. The anti-parallel arrays of such arrangements in the crystal form monolayers of thickness 13.8 Å. The long molecular axis of **1** and is parallel to the (001) direction. The molecules are stacked one on top of the other along the (010)

direction. A view down the *b*-axis reflects the stability afforded by the stacked and parallel arrangement (Fig. 3). Each monolayer may be divided into two regions. The first is a central region containing the flat tetracyclic ring system packed in an orderly arrangement. The second is the peripheral regions of the monolayer characterized by looser packing. In the second region, the packing of the C(17) side-chain with the corresponding 5-bromopentyl side-chain of the adjacent molecules along the *a*-axis and *c*-axis becomes apparent. This type of molecular packing gives a crystal density of 1.188 Mg/m^3.

One possible approach to observe side-chain disorder in this class of molecules would be to compare the crystal structure of the same molecule at different temperatures and observe the induced thermal motion. Upon examination of C–C distances less than 4.5 Å [12] for the structure of **1** determined at 130 K as well as the packing shown in Fig 1C, it is evident that there is a packing of side-chains at C(17) and O(3). For nearest neighbor molecules, C–C distances less than 4.5 Å for C(17) and O(3) side-chain are 38 in number. Interestingly, Br(1) too possesses extremely short contacts with C(16) and C(19) (3.94 and 3.98 Å, respectively) as well as 7 other contacts making it the atom with the largest number of intermolecular contacts in the molecule. The atoms which have the most number of intermolecular

Table 2

Atomic coordinates and equivalent isotropic displacement parameters U_{eq} is defined as one third of the trace of the orthogonalized U_{ij} tensor. (Coordinates are fractional $\times 10^4$; isotropic thermal parameters are U_{eq} ($\text{Å}^2 \times 10^3$). The ESD values are given in parentheses)

	x	y	z	U_{eq}
Br(1)	3805 (1)	8952 (1)	9285 (1)	55 (1)
C(14	−6164 (3)	9104 (5)	15228 (3)	18 (1)
C(16)	−7379 (3)	8955 (6)	16566 (2)	23 (1)
C(10)	−4456 (3)	8756 (5)	12880 (3)	23 (1)
C(13)	−7344 (2)	8954 (5)	14780 (2)	17 (1)
C(9)	−5329 (3)	9333 (4)	13592 (3)	16 (1)
C(3)	−2328 (3)	9619 (5)	12007 (3)	32 (1)
C(7)	−4138 (3)	8789 (5)	15089 (3)	20 (1)
C(11)	−6509 (3)	9329 (4)	13133 (3)	21 (1)
O(3)	−1420 (2)	9368 (4)	11387 (2)	43 (1)
C(1)	−4361 (3)	9873 (5)	12032 (3)	28 (1)
C(12)	−7379 (3)	9852 (5)	13826 (3)	21 (1)
C(8)	−5273 (3)	8535 (4)	14586 (3)	18 (1)
C(29)	533 (4)	9358 (9)	11235 (4)	64 (2)
C(25)	−12475 (4)	9711 (6)	17954 (4)	32 (1)
C(31)	1498 (4)	9213 (10)	9629 (4)	65 (2)
C(6)	−3230 (3)	8658 (4)	14396 (3)	23 (1)
C(2)	−3373 (4)	9597 (6)	11399 (3)	36 (1)
C(19)	−4767 (4)	7207 (5)	12467 (3)	32 (1)
C(20)	−9250 (3)	9249 (5)	15644 (3)	21 (1)
C(5)	−3343 (3)	8623 (4)	13429 (3)	20 (1)
C(24)	−11307 (3)	10126 (6)	17692 (3)	31 (1)
C(15)	−6242 (3)	8463 (4)	16258 (3)	22 (1)
C(21)	−9858 (3)	9761 (6)	14716 (3)	32 (1)
C(17)	−8003 (3)	9576 (4)	15639 (3)	17 (1)
C(27)	−12799 (4)	10590 (6)	18842 (3)	41 (1)
C(26)	−12608 (6)	8067 (8)	18106 (6)	72 (2)
C(18)	−7652 (3)	7327 (5)	14591 (3)	24 (1)
C(30)	548 (4)	9876 (9)	10204 (4)	66 (2)
C(32)	2575 (5)	9854 (8)	9968 (5)	59 (2)
C(4)	−2364 (3)	8438 (5)	1280 7(3)	29 (1)
C(23)	−10873 (3)	9372 (4)	16786 (3)	24 (1)
C(28)	−413 (4)	9969 (9)	11797 (4)	62 (2)
C(22)	−9747 (3)	9976 (5)	16544 (3)	26 (1)

Table 3

Bond lengths (Å) and angles (°)

Br(1)–C(32)	1.973(6)
C(14)–C(8)	1.514(5)
C(14)–C(15)	1.531(5)
C(14)–C(13)	1.547(4)
C(14)–H(14A)	1.00
C(16)–C(15)	1.530(5)
C(16)–C(17)	1.557(5)
C(16)–H(16A)	0.99
C(16)–H(16B)	0.99
C(10)–C(5)	1.528(5)
C(10)–C(19)	1.542(6)
C(10)–C(1)	1.542(6)
C(10)–C(9)	1.561(5)
C(13)–C(18)	1.527(6)
C(13)–C(12)	1.534(5)
C(13)–C(17)	1.555(5)
C(9)–C(8)	1.538(5)
C(9)–C(11)	1.545(5)
C(9)–H(9A)	1.00
C(3)–O(3)	1.440(5)
(3)–C(2)	1.494(6)
C(3)–C(4)	1.527(6)
C(3)–H(3A)	1.00
C(7)–C(6)	1.493(5)
C(7)–C(8)	1.537(5)
C(7)–H(7A)	0.99
C(7)–H(7B)	0.99
C(11)–C(12)	1.526(5)
C(11)–H(11A)	0.99
C(11)–H(11B)	0.99
O(3)–C(28)	1.434(6)
C(1)–C(2)	1.532(6)
C(1)–H(1A)	0.99
C(1)–H(1B)	0.99
C(12)–H(12A)	0.99
C(12)–H(12B)	0.99
C(8)–H(8A)	1.00
C(29)–C(30)	1.488(8)
C(29)–C(28)	1.516(8)
C(29)–H(29A)	0.99
C(29)–H(29B)	0.99
C(25)–C(26)	1.499(8)
C(25)–C(27)	1.516(7)
C(25)–C(24)	1.529(6)
C(25)–H(25A)	1.00
C(31)–C(32)	1.490(8)
C(31)–C(30)	1.545(8)
C(31)–H(31A)	0.99
C(31)–H(31B)	0.99
C(6)–C(5)	1.327(6)
C(6)–H(6A)	0.95
C(2)–H(2A)	0.99
C(2)–H(2B)	0.99
C(19)–H(19A)	0.98

contacts are C(27) and C(31) = C(21) = C(18), which number 8 and 5, respectively. Thus we observe that the atoms that project out of the plane of the molecule (i.e. C(18) and C(21)) as well as the atoms at the tips of the molecular long axis (i.e. Br(1), C(27) and C(31)) are the atoms that are most accessible to the other molecules in the lattice and are hence most stabilized by these contacts. Stabilization provided by these contacts also serves to restrict their motion. This is verified by the fact that at higher temperature, thermal motion of C(27) is expected for such molecules. This atom now

Table 3 (*continued*)

Br(1)–C(32)	1.973(6)
C(19)–H(19B)	0.98
C(19)–H(19C)	0.98
C(20)–C(21)	1.516(6)
C(20)–C(22)	1.541(5)
C(20)–C(17)	1.549(5)
C(20)–H(20A)	1.00
C(5)–C(4)	1.503(6)
C(24)–C(23)	1.527(6)
C(24)–H(24A)	0.99
C(24)–H(24B)	0.99
C(15)–H(15A)	0.99
C(15)–H(15B)	0.99
C(21)–H(21A)	0.98
C(21)–H(21B)	0.98
C(21)–H(21C)	0.98
C(17)–H(17A)	1.00
C(27)–H(27A)	0.98
C(27)–H(27B)	0.98
C(27)–H(27C)	0.98
C(26)–H(26A)	0.98
C(26)–H(26B)	0.98
C(26)–H(26C)	0.98
C(18)–H(18A)	0.98
C(18)–H(18B)	0.98
C(18)–H(18C)	0.98
C(30)–H(30A)	0.99
C(30)–H(30B)	0.99
C(32)–H(32A)	0.99
C(32)–H(32B)	0.99
C(4)–H(4A)	0.99
C(4)–H(4B)	0.99
C(23)–C(22)	1.525(5)
C(23)–H(23A)	0.99
C(23)–H(23B)	0.99
C(28)–H(28A)	0.99
C(28)–H(28B)	0.99
C(22)–H(22A)	0.99
C(22)–H(22B)	0.99
C(8)–C(14)–C(15)	18.8(3)
C(8)–C(14)–C(13)	114.7(3)
C(15)–C(14)–C(13)	103.9(3)
C(8)–C(14)–H(14A)	106.2(2)
C(15)–C(14)–H(14A)	106.2(2)
C(13)–C(14)–H(14A)	106.2(2)
C(15)–C(16)–C(17)	107.3(3)
C(15)–C(16)–H(16A)	110.3(2)
C(17)–C(16)–H(16A)	110.3(2)
C(15)–C(16)–H(16B)	110.3(2)
C(17)–C(16)–H(16B)	110.3(2)
H(16A)–C(16)–H(16B)	108.5
C(5)–C(10)–C(19)	108.1(3)
C(5)–C(10)–C(1)	109.2(3)
C(19)–C(10)–C(1)	109.5(3)
C(5)–C(10)–C(9)	109.5(3)

Table 3 (*continued*)

Br(1)–C(32)	1.973(6)
C(19)–C(10)–C(9)	111.4(3)
C(1)–C(10)–C(9)	109.2(3)
C(18)–C(13)–C(12)	111.1(3)
C(18)–C(13)–C(14)	111.6(3)
C(12)–C(13)–C(14)	106.5(3)
C(18)–C(13)–C(17)	109.9(3)
C(12)–C(13)–C(17)	117.3(3)
C(14)–C(13)–C(17)	99.8(3)
C(8)–C(9)–C(11)	111.5(3)
C(8)–C(9)–C(10)	113.1(3)
C(11)–C(9)–C(10)	113.1(3)
C(8)–C(9)–H(9A)	106.2(2)
C(11)–C(9)–H(9A)	106.2(2)
C(10)–C(9)–H(9A)	106.2(2)
O(3)–C(3)–C(2)	109.1(3)
O(3)–C(3)–C(4)	111.2(4)
C(2)–C(3)–C(4)	110.0(4)
O(3)–C(3)–H(3A)	108.8(2)
C(2)–C(3)–H(3A)	108.8(3)
C(4)–C(3)–H(3A)	108.8(2)
C(6)–C(7)–C(8)	112.3(3)
C(6)–C(7)–H(7A)	109.1(2)
C(8)–C(7)–H(7A)	109.1(2)
C(6)–C(7)–H(7B)	109.1(2)
C(8)–C(7)–H(7B)	109.1(2)
H(7A)–C(7)–H(7B)	107.9
C(12)–C(11)–C(9)	113.9(3)
C(12)–C(11)–H(11A)	108.8(2)
C(9)–C(11)–H(11A)	108.8(2)
C(12)–C(11)–H(11B)	108.8(2)
C(9)–C(11)–H(11B)	108.8(2)
H(11A)–C(11)–H(11B)	107.7
C(28)–O(3)–C(3)	112.1(4)
C(2)–C(1)–C(10)	114.0(4)
C(2)–C(1)–H(1A)	108.8(2)
C(10)–C(1)–H(1A)	108.8(2)
C(2)–C(1)–H(1B)	108.8(3)
C(10)–C(1)–H(1B)	108.8(2)
H(1A)–C(1)–H(1B)	107.6
C(11)–C(12)–C(13)	111.9(3)
C(11)–C(12)–H(12A)	109.2(2)
C(13)–C(12)–H(12A)	109.2(2)
C(11)–C(12)–H(12B)	109.2(2)
C(13)–C(12)–H(12B)	109.2(2)
H(12A)–C(12)–H(12B)	107.9
C(14)–C(8)–C(7)	110.1(3)
C(14)–C(8)–C(9)	110.5(3)
C(7)–C(8)–C(9)	109.5(3)
C(14)–C(8)–H(8A)	108.9(2)
C(7)–C(8)–H(8A)	108.9(2)
C(9)–C(8)–H(8A)	108.9(2)
C(30)–C(29)–C(28)	114.1(5)
C(30)–C(29)–H(29A)	108.7(3)
C(28)–C(29)–H(29A)	108.7(3)

Table 3 (*continued*)

Br(1)–C(32)	1.973(6)
C(30)–C(29)–H(29B)	108.7(5)
C(28)–C(29)–H(29B)	108.7(4)
H(29A)–C(29)–H(29B)	107.6
C(26)–C(25)–C(27)	111.6(5)
C(26)–C(25)–C(24)	112.3(5)
C(26)–C(25)–H(25A)	107.7(5)
C(27)–C(25)–H(25A)	107.7(3)
C(24)–C(25)–H(25A)	107.7(2)
C(32)–C(31)–C(30)	111.2(6)
C(32)–C(31)–H(31A)	109.4(4)
C(30)–C(31)–H(31A)	109.4(4)
C(32)–C(31)–H(31B)	109.4(3)
C(30)–C(31)–H(31B)	109.4(3)
H(31A)–C(31)–H(31B)	108.0
C(5)–C(6)–C(7)	126.0(3)
C(5)–C(6)–H(6A)	117.0(2)
C(7)–C(6)–H(6A)	117.0(2)
C(3)–C(2)–C(1)	110.8(4)
C(3)–C(2)–H(2A)	109.5(3)
C(1)–C(2)–H(2A)	109.5(3)
C(3)–C(2)–H(2B)	109.5(2)
C(1)–C(2)–H(2B)	109.5(2)
H(2A)–C(2)–H(2B)	108.1
C(10)–C(19)–H(19A)	109.5(2)
C(10)–C(19)–H(19B)	109.5(2)
H(19A)–C(19)–H(19B)	109.5
C(10)–C(19)–H(19C)	109.5(2)
H(19A)–C(19)–H(19C)	109.5
H(19B)–C(19)–H(19C)	109.5
C(21)–C(20)–C(22)	110.4(3)
C(21)–C(20)–C(17)	112.6(3)
C(22)–C(20)–C(17)	110.0(3)
C(21)–C(20)–H(20A)	107.9(2)
C(22)–C(20)–H(20A)	107.9(2)
C(17)–C(20)–H(20A)	107.9(2)
C(6)–C(5)–C(4)	121.0(3)
C(6)–C(5)–C(10)	122.9(3)
C(4)–C(5)–C(10)	116.1(3)
C(23)–C(24)–C(25)	116.1(4)
C(23)–C(24)–H(24A)	108.3(2)
C(25)–C(24)–H(24A)	108.3(3)
C(23)–C(24)–H(24B)	108.3(2)
C(25)–C(24)–H(24B)	108.3(2)
H(24A)–C(24)–H(24B)	107.4
C(16)–C(15)–C(14)	103.7(3)
C(16)–C(15)–H(15A)	111.0(2)
C(14)–C(15)–H(15A)	111.0(2)
C(16)–C(15)–H(15B)	111.0(2)
C(14)–C(15)–H(15B)	111.0(2)
H(15A)–C(15)–H(15B)	109.0
C(20)–C(21)–H(21A)	109.5(2)
C(20)–C(21)–H(21B)	109.5(2)
H(21A)–C(21)–H(21B)	109.5
C(20)–C(21)–H(21C)	109.5(2)

Table 3 (*continued*)

Br(1)–C(32)	1.973(6)
H(21A)–C(21)–H(21C)	109.5
H(21B)–C(21)–H(21C)	109.5
C(20)–C(17)–C(13)	118.2(3)
C(20)–C(17)–C(16)	112.0(3)
C(13)–C(17)–C(16)	103.8(3)
C(20)–C(17)–H(17A)	107.4(2)
C(13)–C(17)–H(17A)	107.4(2)
C(16)–C(17)–H(17A)	107.4(2)
C(25)–C(27)–H(27A	109.5(3)
C(25)–C(27)–H(27B)	109.5(3)
H(27A)–C(27)–H(27B)	109.5
C(25)–C(27)–H(27C)	109.5(3)
H(27A)–C(27)–H(27C)	109.5
H(27B)–C(27)–H(27C)	109.5
C(25)–C(26)–H(26A)	109.5(4)
C(25)–C(26)–H(26B)	109.5(4)
H(26A)–C(26)–H(26B)	109.5
C(25)–C(26)–H(26C)	109.5(5)
H(26A)–C(26)–H(26C)	109.5
H(26B)–C(26)–H(26C)	109.5
C(13)–C(18)–H(18A)	109.5(2)
C(13)–C(18)–H(18B)	109.5(2)
H(18A)–C(18)–H(18B)	109.5
C(13)–C(18)–H(18C)	109.5(2)
H(18A)–C(18)–H(18C)	109.5
H(18B)–C(18)–H(18C)	109.5
C(29)–C(30)–C(31)	113.7(5)
C(29)–C(30)–H(30A)	108.8(5)
C(31)–C(30)–H(30A)	108.8(4)
C(29)–C(30)–H(30B)	108.8(3)
C(31)–C(30)–H(30B)	108.8(3)
H(30A)–C(30)–H(30B)	107.7
C(31)–C(32)–Br(1)	111.8(4)
C(31)–C(32)–H(32A)	109.3(3)
Br(1)–C(32)–H(32A)	109.3(2)
C(31)–C(32)–H(32B)	109.3(4)
Br(1)–C(32)–H(32B)	109.3(2)
H(32A)–C(32)–H(32B)	107.9
C(5)–C(4)–C(3)	112.2(3)
C(5)–C(4)–H(4A)	109.2(2)
C(3)–C(4)–H(4A)	109.2(2)
C(5)–C(4)–H(4B)	109.2(2)
C(3)–C(4)–H(4B)	109.2(2)
H(4A)–C(4)–H(4B)	107.9
C(22)–C(23)–C(24)	111.4(3)
C(22)–C(23)–H(23A)	109.4(2)
C(24)–C(23)–H(23A)	109.4(2)
C(22)–C(23)–H(23B)	109.4(2)
C(24)–C(23)–H(23B)	109.4(2)
H(23A)–C(23)–H(23B)	108.0
O(3)–C(28)–C(29)	108.8(5)
O(3)–C(28)–H(28A)	109.9(3)
C(29)–C(28)–H(28A)	109.9(3)
O(3)–C(28)–H(28B)	109.9(4)

Table 3 (*continued*)

Br(1)–C(32)	1.973(6)
C(29)–C(28)–H(28B)	109.9(4)
H(28A)–C(28)–H(28B)	108.3
C(23)–C(22)–C(20)	114.2(3)
C(23)–C(22)–H(22A)	108.7(2)
C(20)–C(22)–H(22A)	108.7(2)
C(23)–C(22)–H(22B)	108.7(2)
C(20)–C(22)–H(22B)	108.7(2)
H(22A)–C(22)–H(22B)	107.6

Table 4

Anisotropic displacement parameters ($\text{Å}^2 \times 10^3$). The anisotropic displacement factor exponent takes the form: $-2\pi^2[h^2 a^* U_{11} + \cdots + 2hka^*b^* U_{12}]$

	U_{11}	U_{22}	U_{33}	U_{23}	U_{13}	U_{12}
Br(1)	44(1)	71(1)	50(1)	6(1)	11(1)	−2(1)
C(14)	10(2)	20(2)	24(2)	3(2)	1(1)	−1(2)
C(16)	15(2)	30(2)	23(2)	0(2)	2(1)	4(2)
C(10)	17(2)	28(2)	23(2)	−3(2)	1(1)	1(2)
C(13)	9(2)	20(2)	23(2)	−1(2)	1(1)	5(2)
C(9)	10(2)	19(2)	19(2)	−3(1)	1(1)	2(1)
C(3)	22(2)	49(3)	28(2)	−2(2)	13(2)	1(2)
C(7)	11(2)	25(2)	25(2)	2(2)	−2(1)	−1(2)
C(11)	13(2)	31(2)	20(2)	0(2)	−1(1)	0(2)
O(3)	27(2)	70(3)	32(2)	0(2)	16(1)	1(2)
C(1)	21(2)	41(3)	22(2)	−3(2)	4(2)	4(2)
C(12)	12(2)	27(2)	25(2)	−2(2)	−2(2)	0(2)
C(8)	10(2)	16(2)	27(2	−2(1)	−3(2)	0(1)
C(29)	23(2)	123(7)	46(3)	21(3)	8(2)	−5(3)
C(25)	23(2)	46(3)	25(2)	1(2)	6(2)	5(2)
C(31)	54(3)	105(6)	37(3)	−6(3)	10(2)	−9(4)
C(6)	7(2)	27(2)	35(2)	2(2)	2(2)	1(2)
C(2)	30(2)	52(3)	26(2)	1(2)	10(2)	5(2)
C(19)	23(2)	36(2)	38(3)	−18(2)	5(2)	4(2)
C(20)	10(2)	29(2)	25(2)	−5(2)	6(1)	−3(2)
C(5)	16(2)	17(2)	27(2)	−2(2)	2(2)	−2(2)
C(24)	21(2)	48(3)	25(2)	−6(2)	0(2)	2(2)
C(15)	15(2)	28(2)	24(2)	5(2)	0(2)	2(2)
C(21)	11(2)	51(3)	33(2)	−2(2)	5(2)	4(2)
C(17)	13(2)	20(2)	18(2)	−1(2)	5(2)	1(1)
C(27)	27(2)	70(3)	26(2)	2(2)	7(2)	8(2)
C(26)	69(4)	55(4)	94(5)	0(4)	56(4)	−2(3)
C(18)	14(2)	27(2)	29(2)	−6(2)	2(2)	−1(2)
C(30)	31(3)	122(6)	44(3)	13(3)	4(2)	11(3)
C(32)	61(4)	67(4)	49(3)	−4(3)	12(3)	5(3)
C(4)	15(2)	38(3)	35(2)	−1(2)	4(2)	2(2)
C(23)	17(2)	28(2)	28(2)	−1(2)	5(2)	2(2)
C(28)	30(3)	119(5)	37(3)	−1(3)	2(2)	−19(3)
C(22)	18(2)	35(2)	24(2)	−3(2)	1(2)	3(2)

Table 5

Hydrogen coordinates and isotropic displacement parameters ($\text{Å}^2 \times 10^3$). (Coordinates are fractional $\times 10^4$; isotropic thermal parameters are U_{eq} ($\text{Å}^2 \times 10^3$). The ESD values are given in parentheses)

	x	y	z	U_{eq}
H(14A)	−6028(3)	10197(5)	15312(3)	22
H(16A)	−7310(3)	9736(6)	17075(2)	27
H(16B)	−7782(3)	8099(6)	16833(2)	27
H(9A)	−5143(3)	10400(4)	13728(3)	20
H(3A)	−2241(3)	10622(5)	12319(3)	39
H(7A)	−4118(3)	9795(5)	15388(3)	24
H(7B)	−4023(3)	8050(5)	15620(3)	24
H(11A)	−6532(3)	9983(4)	12550(3)	25
H(11B)	−6692(3)	8306(4)	12911(3)	25
H(1A)	−5040(3)	9823(5)	11612(3)	33
H(1B)	−4307(3)	10893(5)	12305(3)	33
H(12A)	−8114(3)	9749(5)	13499(3)	25
H(12B)	−7260(3)	10919(5)	13979(3)	25
H(8A)	−5382(3)	7441(4)	14478(3)	21
H(29A)	1231(4)	9654(9)	11576(4)	76
H(29B)	496(4)	8256(9)	11241(4)	76
H(25A)	−12979(4)	10010(6)	17394(4)	38
H(31A)	1514(4)	8118(10)	9717(4)	78
H(31B)	1369(4)	9423(10)	8924(4)	78
H(6A)	−2504(3)	8592(4)	14672(3)	28
H(2A)	−3456(4)	8619(6)	11070(3)	43
H(2B)	−3348(4)	10376(6)	10889(3)	43
H(19A)	−5480(4)	7267(5)	12111(3)	48
H(19B)	−4813(4)	6493(5)	13005(3)	48
H(19C)	−4207(4)	6877(5)	12021(3)	48
H(20A)	−9348(3)	8146(5)	15699(3)	25
H(24A)	−11276(3)	11218(6)	17596(3)	38
H(24B)	−10806(3)	9881(6)	18257(3)	38
H(15A)	−6182(3)	7363(4)	16251(3)	27
H(15B)	−5659(3)	8874(4)	16704(3)	27
H(21A)	−9533(3)	9291(6)	14151(3)	47
H(21B)	−9800(3)	10847(6)	14660(3)	47
H(21C)	−10633(3)	9477(6)	14739(3)	47
H(17A)	−7910(3)	10684(4)	15643(3)	21
H(27A)	−12703(4)	11657(6)	18719(3)	61
H(27B)	−12335(4)	10293(6)	19410(3)	61
H(27C)	−13570(4)	10389(6)	18972(3)	61
H(26A)	−12392(6)	7533(8)	17520(6)	107
H(26B)	−13377(6)	7845(8)	18230(6)	107
H(26C)	−12141(6)	7748(8)	18667(6)	107
H(18A)	−7624(3)	6779(5)	15210(3)	35
H(18B)	−7133(3)	6883(5)	14147(3)	35
H(18C)	−8396(3)	7274(5)	14295(3)	35
H(30A)	608(4)	10976(9)	10198(4)	79
H(30B)	−158(4)	9605(9)	9866(4)	79
H(32A)	2684(5)	9686(8)	10679(5)	70
H(32B)	2568(5)	10943(8)	9852(5)	70
H(4A)	−2388(3)	7437(5)	12503(3)	35
H(4B)	−1685(3)	8504(5)	13228(3)	35

Table 5 (*continued*)

	x	y	z	U_{eq}
H(23A)	−10820(3)	8284(4)	16900(3)	29
H(23B)	−11395(3)	9541(4)	16224(3)	29
H(28A)	−324(4)	9686(9)	12494(4)	74
H(28B)	−426(4)	11070(9)	11754(4)	74
H(22A)	−9237(3)	9823(5)	17117(3)	31
H(22B)	−9809(3)	11062(5)	16430(3)	31

destabilizes all atoms like O(3), Br(1), C(19) and C(31) that make intermolecular contacts with it. These atoms, in turn, experience a greater freedom and destabilize their intermolecular contacts. This has a telling effect on the second region of the monolayer where the packing of the side-chains is grossly disturbed all along the length of the side chain. Thus at 298 K, although the tetracyclic ring system remains unaffected, C(32), C(31), C(30), C(26) and C(27) showed a smearing of electron density resisting a complete solution of the crystal (Tables 2–5).

In order to probe the effect of chain length of the *O*-alkyl segment on the thermal motions under the same conditions of temperature in this class of molecules, an analogous compound **2** with longer chain [Br(CH₂)₁₁–] at the ether link of cholesteryl system was synthesized and investigated. The X-ray diffraction data showed that for **2** even at 130 K (not shown), thermal motions showed a smearing of electron density of the C(17) side chain (i.e. C(26) and C(27)) and the 11-bromoundecanoyl chain at O(3). Interestingly, the tetracyclic system of the steroid is nicely resolved at 130 K showing much less thermal motion even compared to bromine, which is attached to the side-chain indicating that there is actually thermal motion and not static disorder in the crystal. Although the effective length of the steroid is largely conserved (9.007 Å), there is a drastic reduction in the degree of twist of the ring system, which is only 2.4°. In fact, in related structures this angle varies from 7.9 to 15° [26]. The atoms C(4), C(5), C(6), C(7) and C(10) are part of the same plane containing the ethylenic group of the cholesterol moiety in the three determined crystal structures. Table 6 gives the best least square planes for selected groups of atoms. Also, the length of the *a*- and *b*-axes of **2** at 130 K are conserved (i.e. 12.709 and 8.9 Å in **2**) while the that of the *c*-axis increases by 3.0 Å (16.727 Å) as

compared to the axes of **1** at 298 and 130 K. A similar mode of packing of molecules **1** and **2** is consistent with an increase in length of the *c*-axis with increase in length of alkyl chain at O(3).

Another means of examining side chain motion or the stabilization due to packing of the side chains in the peripheral region of the monolayer would be to compare **1** and **2** (which differ only in the length of *n*-alkyl segment) at the same temperature (i.e. 130 K). In contrast, the conformational details of the side chain at O(3) for **1** could be determined. Remarkably, the *n*-pentyl side chain in **1** crystallizes in an alternating s-*gauche* and s-*trans* conformation (Fig. 1A), which is rather rare [27,28]. Segments containing *n*-alkyl chain generally tend to crystallize in an all-s-*trans* conformation. This unusual conformation seems to be stabilized in this molecule by interaction with the alkyl side-chain at C(17) of the adjacent steroid molecule. Increase in temperature results in thermal motion of this side-chain as well as the terminal methyl group (C(27)) of the side-chain at C(17), which results in the disruption of packing at the peripheral regions of the monolayer. Since the packing is based on an anti-parallel arrangement of adjacent molecules, the extra stabilization presumably originates from the packing of the side-chains at O(3) and C(17). Possibly an optimal length of alkyl segment at O(3) is required for the maximum efficient intermolecular contacts for both side-chains. While the side-chain at C(17) remains always in its fully extended conformation, in **1**, the side-chain at O(3) in its fully extended conformation would be slightly more than the afore-mentioned optimal length. The introduction of a kink,

Table 6
Best least-squares planes calculated for selected groups of atoms. (The planes are (1) the tetracyclic ring system of the steroid i.e. C(1)–C(17); (2) the ethylenic group i.e. C(5), C(6), C(10), C(4) and C(7). Equations are in the form $ax + by + cz = d$ referred to as crystallographic axes. The plane constants are in Å)

Plane	Structure	a	b	c	d
(1)	**A**	−0.184	0.951	−0.250	0.098
	B	0.174	0.963	0.204	10.73
	C	0.182	0.958	0.125	7.69
(2)	**A**	−0.117	0.993	0.003	3.16
	B	0.105	0.994	−0.028	6.75
	C	0.035	0.999	−0.014	6.14

or a s-*gauche* conformation in an alkyl chain shortens it by 1.2 Å [29]. Hence it collapses spontaneously to a slightly shorter alternate *gauche–trans* conformation to attain an optimal chain length match in order to achieve these contacts along the maximum possible distance. Introduction of a longer polymethylene chain as in **2** results in a 3 Å increase in the *c*-axis indicating that a substantial portion of the side chain juts out beyond the length of the C(17) side chain. This portion of the O(3) alkyl chain possesses increased mobility due to lack of sufficient interaction with the adjacent C(17) chain due to a chain length mismatch between the two alkyl segments at C(17) and O(3). The flexibility so experienced is now transmitted to the entire length of the side chain at O(3) that can no longer pack effectively with the C(17) side chain. This motion in turn gets translated all along the chain length for both side chains in **2** at 130 K. This is reflected in the incomplete solution of the crystal structure of **2** even at 130 K.

Thus, the effect of temperature on a given length of side-chain as well as the effect of the length of the side-chain at a given temperature on thermal motions in this class of molecules have been investigated. It may be possible that this unusual tendency of kink formation with ether-bearing hydrocarbon chain of cationic cholesteryl amphiphiles might make them better candidates for gene delivery.

Acknowledgements

References

[1] S. Bhattacharya, S. De, Chem. Eur. J. 5 (1999) 2335.

[2] S. Bhattacharya, S.S. Mandal, Biochim. Biophys. Acta 1323 (1997) 29.

[3] Y. Krishnan-Ghosh, S.S. Visveswariah, S. Bhattacharya, FEBS Lett. 473 (2000) 341.

[4] M.R. Vist, J.H. Davis, Biochemistry 29 (1990) 451.

[5] M.B. Sankaram, T.E. Thompson, Biochemistry 29 (1990) 10676.

[6] R.A. Demel, A.K. Lala, S. Nanda Kumari, L.L.M. Van Deenen, Biochim. Biophys. Acta 771 (1984) 142.

[7] K.R. Patel, M.P. Li, J.R. Schuh, J.D. Baldeschweiler, Biochim. Biophys. Acta 814 (1985) 256.

[8] E.S. Meadows, E. Abel-Santos, D.C. Frankel, G.W. Gokel, Tetrahedron Lett. 41 (2000) 1871.

[9] Y. Krishnan-Ghosh, S.S. Indi, S. Bhattacharya, unpublished work.

[10] S.L. De Wall, K. Wang, D.R. Berger, S. Watanabe, J.C. Hernandez, G.W. Gokel, J. Org. Chem. 62 (1997) 6784.

[11] E.J. Dufourc, E.J. Parish, S. Chitrakorn, I.C.P. Smith, Biochemistry 23 (1984) 6062.

[12] P. Sawzik, B.M. Craven, Acta Cryst. B 36 (1980) 3027.

[13] J.A.W. Barnard, J.E. Lydon, Mol. Cryst. Liq. Cryst. 26 (1974) 285.

[14] S. Abrahamsson, B. Dahlén, J. Chem. Soc. Chem. Commun. (1976) 117.

[15] J.H. Wendorff, F.P. Price, Mol. Cryst. Liq. Cryst. 22 (1973) 85.

[16] G. Jones, A. Rosenthal, D. Segev, Y. Mazur, F. Frolow, Y. Halfon, D. Rabinovich, Z. Shakked, Tetrahedron Lett. 2 (1979) 177.

[17] E. Galdecka, Z. Galdecki, Z. Górkiewicz, A. Kurek-Tyrlik, F.Z. Makaev, J. Wicha, J. Calverly, Pol. J. Chem. 73 (1999) 547.

[18] M.K. Yun, Y.J. Park, W. Shin, B.M. Craven, Bull. Korean Chem. Soc. 10 (1989) 335.

[19] D.A. Perrin, W.L. Armarego, D.R. Perrin, Purification of Laboratory Chemicals, 3rd Ed., Pergamon Press, New York, 1990.

[20] S.C. Davis, F.C. Szoka Jr., Bioconjugate Chem. 9 (1998) 783.

[21] SIEMENS Analytical X-ray Instruments Inc., Madison, Wisconsin, USA, 1995.

[22] SHELXTL (SGI version) SIEMENS Analytical X-ray Instruments Inc., Madison, Wisconsin, USA, 1995.

[23] V. Schomaker, K.N. Trueblood, Acta Cryst. B 24 (1968) 63.

[24] P. Sawzik, B.M. Craven, Acta Cryst. B 35 (1979) 895.

[25] S.C. Nyburg, Acta Cryst. B 30 (1974) 251.

[26] V. Pattabhi, B.M. Craven, J. Lipid Res. 20 (1979) 753.

[27] H. Hartung, U. Baumeiter, F. Thielemann, M. Jaskolski, Acta Cryst. C 39 (1984) 482.

[28] V.N. Belov, C. Funke, T. Labahn, M. Es-Sayed, A. de Meijere, Eur. J. Org. Chem. (1999) 1345.

[29] H. Scherr, P.C. Hagele, H.P. Grossmann, Colloid Polym. Sci. 252 (1974) 871.